Int. J. Solids Structures Vol. 30, No. 18, pp. 2469–2484, 1993
Printed in Great Britain

0020-7683/93 $6.00+ .00
Pergamon Press Ltd

ANALYTICAL DETERMINATION OF CONTACT STRESSES IN MECHANICALLY FASTENED COMPOSITE LAMINATES WITH FINITE BOUNDARIES

E. MADENCI and L. ILERI
Department of Aerospace and Mechanical Engineering, The University of Arizona, Tucson, AZ 85721, U.S.A.

(*Received* 15 *July* 1992; *in revised form* 19 *March* 1993)

Abstract—The present analysis focuses on the assessment of the contact stresses in mechanical joints with a single fastener, with two fasteners, and with a row of fasteners perpendicular to loading in finite composite laminates. The solution is obtained by solving the governing equations of elasticity under plane-stress assumptions using the modified mapping-collocation method. The load exerted by the fastener through the contact region, which consists of no-slip and slip zones due to the presence of friction, is modeled with appropriate mixed boundary conditions. The analysis results compare favorably with the photoelastic experimental measurements available in the literature.

1. INTRODUCTION

Mechanical fasteners, such as bolts or pins, are a prime means of load transfer in composite structures. However, they give rise to stress concentrations and are often the source and location of static and fatigue failures. The presence of the unknown contact stress distribution and the contact region between the pin and the composite laminate, as well as the anisotropy of the material, results in a complex non-linear problem. In view of the critical nature of mechanically fastened composite components, determination of accurate stress distribution becomes essential for reliable failure prediction.

A considerable amount of work on the behavior of mechanically fastened joints has been reported in the literature. These studies investigated the stress distribution around a pin-loaded hole in laminated composites based on either finite element analysis or analytical methods. Since the contact stress distribution and the contact region are not known *a priori*, the majority of the models did not directly impose the boundary conditions appropriate for modeling the contact and non-contact regions between the fastener and the boundary of the hole. These models usually assumed a cosinusoidal bearing stress distribution or zero radial displacements over the hole boundary.

The finite element modeling of single-fastener joints with appropriate boundary conditions can be grouped into two categories: direct and inverse methods. The models based on the direct method utilize an incremental finite element formulation with an iterative solution procedure because of the non-linear nature of the problem. This method was successfully used by Wilkinson *et al.* (1981), Rowlands *et al.* (1982) and Rahman *et al.* (1984) for determining the contact stresses around pin-loaded holes, considering the effects of friction and material orthotropy. With this method, Eriksson (1986) examined the effect of bolt rigidity, as well as clearance, friction and the elastic laminate properties. Eriksson also confirmed the conclusion reported by Hyer and Klang (1985) by showing that pin flexibility is not a significant variable in determining contact stresses along the hole boundary. Marshall *et al.* (1989) conducted a three-dimensional finite element analysis of pin-loaded holes to show the effect of pin-hole contact friction, laminate stiffness and clamping force on the interlaminar stresses. More recently, Murthy *et al.* (1990) introduced an improved iterative finite element solution to study the eccentrically located single-fastener joints. The main drawback of the direct method is that it requires an iterative solution procedure; this usually leads to convergence difficulties and high computational costs.

The inverse method requires a linear finite element analysis, with conditions along the pin-hole contact region specified as displacement constraint equations. The major

shortcoming of this method is that the variation of the contact region as a function of the applied load should be known *a priori*. Furthermore, this method becomes inadequate for problems involving material anisotropy and asymmetry. The concept of the inverse method was introduced by Eshwar (1978). Mangalgiri *et al.* (1984), Naik and Crews (1986, 1991) and Ramamurthy (1989) incorporated this concept into the finite element analysis to investigate single-fastener joints. These models did not account for the effects of friction, material anisotropy and non-symmetric configurations.

Among all the analytical studies, the one by Hyer and Klang (1985) is the only one that included the interfacial boundary conditions appropriate for modeling the contact problem between the fastener and the hole boundary in an infinitely large orthotropic laminate. Their analysis was based on a complex variable formulation introduced by Lekhnitskii (1968). Hyer and Klang examined the effects of friction, pin rigidity and clearance in detail. Within the two-dimensional theory of elasticity, they concluded that pin flexibility is not a significant variable in determining contact stresses along the hole boundary. However, they established that the often-assumed cosinusoidal bearing stress distribution is not accurate and that the contact stresses are influenced significantly by the material anisotropy, friction and pin-hole clearance.

In all of the analytical studies, except for Oplinger and Gandhi (1974), the pin-loaded laminate was taken to be infinitely large based on the assumption that the fasteners were not too close to one another, or to a neighboring free surface. Therefore, they could not account for the effect of finite geometry of the laminate and the interaction of adjacent fasteners. In order to capture the effect of finite geometry, Oplinger and Gandhi incorporated the Modified-Mapping Collocation (MMC) method introduced by Bowie and Neal (1970) into Lekhnitskii's (1968) formulation. However, their study is limited to the analysis of a pin-loaded hole configuration that requires both geometric and material symmetry conditions. Also, they did not include the effect of friction between the fastener and the hole boundary.

The present analytical study eliminates these shortcomings by extending the recent formulation of the MMC method presented by Madenci *et al.* (1993). Section 2 presents the mathematical modeling of the problem for two-dimensional analysis within the theory of elasticity. The solution method based on the MMC technique is described in Section 3. Section 4 presents the numerical results for a finite geometry anisotropic laminate with a single pin-loaded hole and for a finite geometry orthotropic laminate with two pin-loaded holes positioned side by side. Section 4 also includes numerical results describing the effect of spacing between the multiple pin-loaded holes aligned perpendicular to the load in an orthotropic laminate.

2. PROBLEM STATEMENT

This study addresses the determination of contact stresses in laminated anisotropic composites due to the presence of rigid mechanical fasteners without any clamping over the washer area. Mechanical joints with a single fastener, with two fasteners parallel to each other, and with a row of fasteners perpendicular to loading are considered (Fig. 1). In the case of a single fastener, Fig. 2 describes the configuration of a pin-loaded hole before and after the finite anisotropic laminate is subjected to uniaxial loading.

A Cartesian coordinate system (x, y) and a polar coordinate system (r, θ) are employed whose origins coincide with the center of the pin-loaded hole. The hole radius, a, is taken to be unity so that the problem statement is in dimensionless form. The pin radius, R, is assumed to be slightly smaller than the radius of the hole, resulting in a pin-hole clearance denoted by λ.

The length and width of the finite rectangular region are denoted by L and H, respectively. The off-centered position of the pin in relation to the boundaries of the finite region is specified by l and h.

Each lamina considered in this study is composed of homogeneous, elastic and orthotropic material with elastic moduli, E_L and E_T; shear modulus, G_{LT}; and Poisson's ratio, ν_{LT}, where L and T are the longitudinal and transverse directions relative to the fibers in

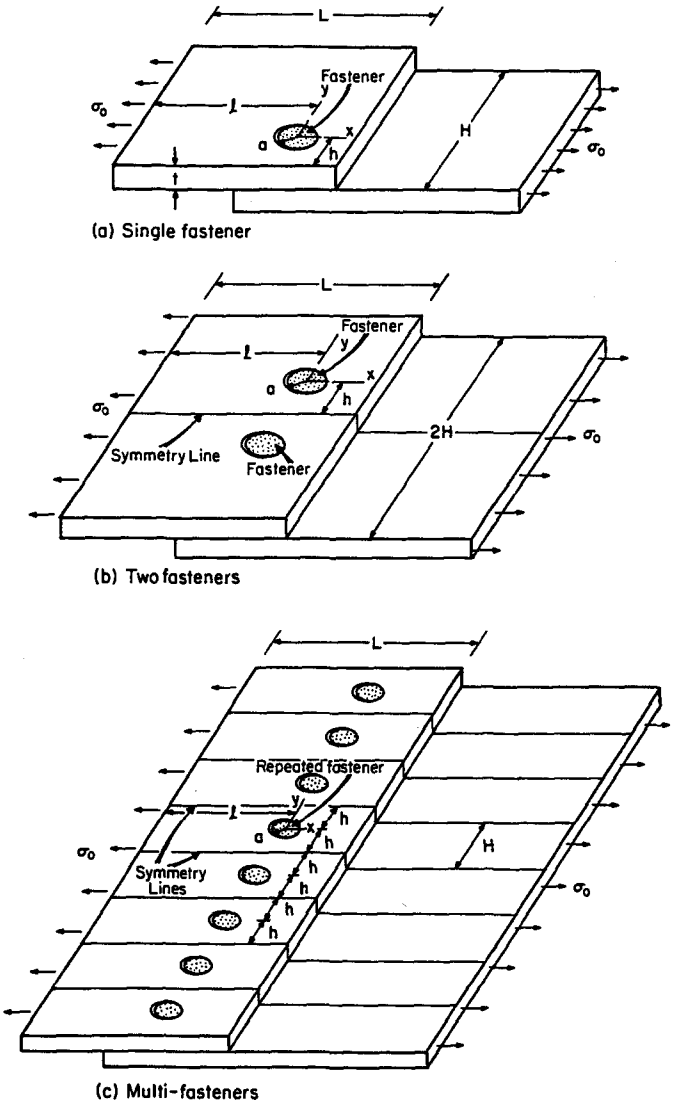

Fig. 1. Mechanically fastened composite laminate configurations under consideration.

the lamina. However, the composite laminate is considered to be anisotropic and homogeneous with compliance coefficients, a_{ij}.

As the laminate is subjected to uniform stress, σ_0, along the $x = -l$ plane, the contact region, whose extent is not known, develops between the fastener and the hole boundary. The fastener exerts loading on the hole boundary through this contact region, which consists of no-slip and slip zones due to the presence of friction. The boundary conditions associated with the slip zone involve the Coulomb friction model with a coefficient of friction, f. The no-slip and slip zones of the hole boundary are described by P and S as

$$P = \{r, \theta : r = a, \theta \in (-\psi_1, \eta_1)\}$$
$$S = \{r, \theta : r = a, \theta \in [-(\psi_2 - \psi_1), (\eta_2 - \eta_1)]\}.$$

The remaining portion of the hole boundary, which is free of traction, becomes

$$Q = \{r, \theta : r = a, \theta \in (\eta_2, -\psi_2)\}.$$

These boundary conditions are expressed as:

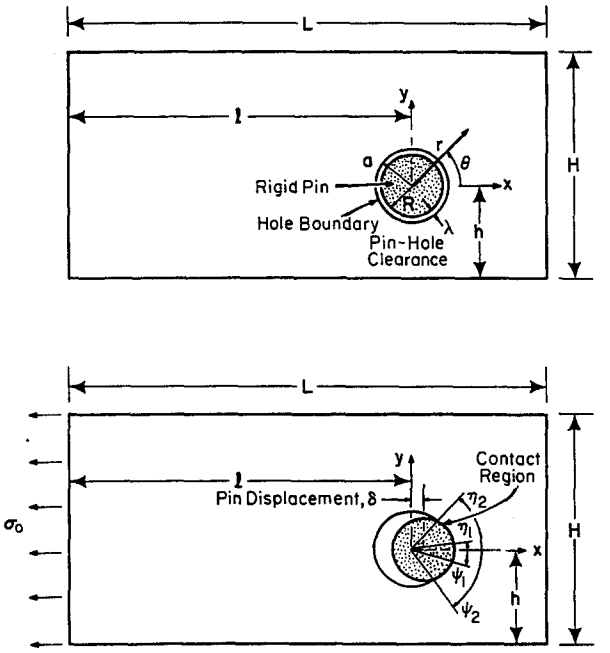

Fig. 2. Mechanically fastened composite laminate with finite dimensions, before and after loading.

$$
\begin{aligned}
u_r(a,\theta) &= -(\delta\cos\theta-\lambda) && \text{on surfaces } P \text{ and } S\\
u_\theta(a,\theta) &= -\delta\sin\theta && \text{on surface } P\\
|\sigma_{r\theta}(a,\theta)| &= f|\sigma_{rr}(a,\theta)| && \text{on surface } S\\
\left.\begin{aligned}\sigma_{rr}(a,\theta)&=0\\ \sigma_{r\theta}(a,\theta)&=0\end{aligned}\right\} && \text{on surface } Q
\end{aligned}
\tag{1}
$$

in which δ corresponds to the displacement of the rigid pin. The components of the displacement and stress fields referenced to the polar coordinates (r,θ) are denoted by u_r and u_θ, and σ_{rr}, $\sigma_{\theta\theta}$ and $\sigma_{r\theta}$, respectively.

The angles η_1, η_2, ψ_1 and ψ_2 defining the no-slip and slip zones described by surfaces P and Q are determined from additional conditions:

$$
\begin{aligned}
&a\int_0^{2\pi}[-\sigma_{rr}(a,\theta)\cos\theta+\sigma_{r\theta}(a,\theta)\sin\theta]\,d\theta-\sigma_0 H=0\\
&a\int_0^{2\pi}[-\sigma_{rr}(a,\theta)\sin\theta+\sigma_{r\theta}(a,\theta)\cos\theta]\,d\theta=0\\
&\sigma_{rr}(a,\theta)<0 \quad \text{on surfaces } P \text{ and } S\\
&\sigma_{rr}(a,\eta_2)=0 \quad \text{and} \quad \sigma_{rr}(a,\psi_2)=0\\
&|\sigma_{r\theta}(a,\eta_1^-)-\sigma_{r\theta}(a,\eta_1^+)|=0\\
&|\sigma_{r\theta}(a,\psi_1^-)-\sigma_{r\theta}(a,\psi_1^+)|=0.
\end{aligned}
\tag{2}
$$

The superscripts $-$ and $+$ indicate whether the angles η_1 and ψ_1 are in the no-slip or slip zones.

By enforcing the appropriate symmetry conditions, shown in Fig. 1(b), contact stresses are obtained for mechanical joints with two rigid fasteners positioned side by side in a finite geometry orthotropic laminate. In the case of multiple rigid fasteners aligned perpendicular

to the loading in an orthotropic laminate as illustrated in Fig. 1(c), contact stresses are determined by considering a representative single fastener subjected to certain symmetry conditions.

The solutions to these non-linear contact problems lead to the determination of the no-slip and slip zones, as well as the contact stress distribution around the pin-loaded hole boundary, while capturing the effect of neighboring free boundaries and the interaction of adjacent fasteners in laminated composites.

3. SOLUTION METHOD

Under plane stress assumptions within the theory of elasticity, Lekhnitskii (1968) developed a solution procedure with two analytic functions, $\Phi_1(z_1)$ and $\Phi_2(z_2)$, satisfying the equations of equilibrium and compatibility in Cartesian coordinates (x, y) for anisotropic laminates. The variables z_1 and z_2 are complex and are given by $z_1 = x+\mu_1 y$ and $z_2 = x+\mu_2 y$. The complex parameters μ_1 and μ_2 are the roots of the characteristic equation derived by Lekhnitskii,

$$a_{11}\mu^4 - 2a_{16}\mu^3 + (2a_{12}+a_{66})\mu^2 - 2a_{66}\mu + a_{22} = 0 \tag{3}$$

in which a_{ij} $(i, j = 1, 2, 6)$ are the compliance coefficients of a laminate.

The stress and displacement components can be expressed as

$$\begin{aligned}
\sigma_{xx} &= 2\,\mathrm{Re}\,[\mu_1^2\Phi_1'(z_1)+\mu_2^2\Phi_2'(z_2)] \\
\sigma_{yy} &= 2\,\mathrm{Re}\,[\Phi_1'(z_1)+\Phi_2'(z_2)] \\
\sigma_{xy} &= -2\,\mathrm{Re}\,[\mu_1\Phi_1'(z_1)+\mu_2\Phi_2'(z_2)] \\
u_x &= 2\,\mathrm{Re}\,[p_1\Phi_1(z_1)+p_2\Phi_2(z_2)] - \omega y + u_x^0 \\
u_y &= 2\,\mathrm{Re}\,[q_1\Phi_1(z_1)+q_2\Phi_2(z_2)] + \omega x + u_y^0
\end{aligned} \tag{4}$$

where p_k and q_k $(k = 1, 2)$ are given by

$$\begin{aligned}
p_k &= a_{11}\mu_k^2 + a_{12} - a_{16}\mu_k \\
q_k &= a_{12}\mu_k + a_{22}/\mu_k - a_{26}
\end{aligned} \tag{5}$$

and the prime denotes differentiation with respect to the corresponding argument. The rigid-body rotation and displacements are denoted by ω and u_x^0 and u_y^0, respectively.

Determination of the stress and displacement components requires the explicit form of the analytic functions $\Phi_1(z_1)$ and $\Phi_2(z_2)$, such that the specified boundary conditions are satisfied. Thus, these analytic functions are assumed to be in the series form in terms of the mapping functions ξ_1 and ξ_2:

$$\begin{aligned}
\Phi_1(\xi_1) &= \alpha_0 \ln \xi_1 + \sum_{n=1}^{N} (\alpha_{-n}\xi_1^{-n} + \alpha_n \xi_1^n) \\
\Phi_2(\xi_2) &= \beta_0 \ln \xi_2 + \sum_{n=1}^{N} (\beta_{-n}\xi_2^{-n} + \beta_n \xi_2^n).
\end{aligned} \tag{6}$$

The mapping functions, ξ_1 and ξ_2, given by Lekhnitskii (1968) are employed:

$$\xi_k = \frac{z_k \mp \sqrt{z_k^2 - a^2(1+\mu_k^2)}}{a(1-\mathrm{i}\mu_k)} \quad k = 1, 2 \tag{7}$$

where $\mathrm{i} = \sqrt{-1}$ and a is the radius of the hole.

The unknown coefficients, α_i and β_i, in eqn (6) are determined by enforcing conditions (1)–(2) and the requirements for single-valued displacement. The conditions specified by eqn (2) are satisfied through the iterative scheme outlined in detail in Appendix A.

The traction boundary conditions are imposed through resultant forces, $F_x(s)$ and $F_y(s)$, which are expressed in terms of the traction components X_n and Y_n, per unit thickness, acting along the $(s-s_p)$ arc of the boundary B_e and B_i of the laminate (Figure 3):

$$F_x(s) = \int_{s_p}^{s} X_n \, ds; \quad F_y(s) = \int_{s_p}^{s} Y_n \, ds. \tag{8}$$

The parameter s_p indicates an arbitrary point (x_p, y_p) on the boundary, and s is an arc length parameter measured in the counterclockwise direction from s_p.

The components of the resultant forces, F_x and F_y, in terms of the analytic functions, become

$$\begin{aligned} \pm F_x(s) &= 2\,\mathrm{Re}\,[\mu_1\Phi_1(z_1)+\mu_2\Phi_2(z_2)]-2\,\mathrm{Re}\,[\mu_1\Phi_1(z_1^p)+\mu_2\Phi_2(z_2^p)] \\ \mp F_y(s) &= 2\,\mathrm{Re}\,[\Phi_1(z_1)+\Phi_2(z_2)]-2\,\mathrm{Re}\,[\Phi_1(z_1^p)+\Phi_2(z_2^p)]. \end{aligned} \tag{9}$$

Upper and lower signs refer to the exterior and interior boundaries, respectively, and $z_1^p = x_p+\mu_1 y_p$ and $z_2^p = x_p+\mu_2 y_p$.

In order to determine the finite number $(4N+2)$ of unknown coefficients in the series given by eqn (6), M number of collocation points on the boundary are selected for imposing the boundary conditions.† The resulting overdetermined algebraic equations are solved by means of the single value decomposition technique as described by Horn and Johnson (1991). Once the coefficients are determined, the stresses and displacements can be calculated using eqn (4).

4. NUMERICAL RESULTS

This study presents the contact stresses around a pin-loaded hole for three different configurations (Fig. 1). Apart from the boundary conditions along the exterior boundaries, all three configurations involve the same boundary conditions for modeling the load exerted by the rigid fastener on the interior boundary.

Single-fastener analysis

In order to capture the effect of neighboring free boundaries, the first configuration illustrated in Fig. 1(a) involves a single fastener, which is located off-center in a finite geometry anisotropic laminate. The finite laminate is subjected to uniform tractions, σ_0, along the part of the exterior boundary defined by the $x = -l$ line. The boundary conditions associated with the collocation points shown in Fig. 3 are expressed as:

$$\begin{aligned} &F_x = 0, \quad F_y = 0: && m\in[1, K_1] \\ &F_x = 0, \quad F_y = \sigma_0(H-y_p): && m\in[K_1+1, K_2] \\ &F_x = \sigma_0(s_m-y_p), \quad F_y = 0: && m\in[K_2+1, K_3] \\ &F_x = 0, \quad F_y = \sigma_0(-h-y_p): && m\in[K_3+1, K_4] \end{aligned} \tag{10}$$

† Based on a detailed convergence study, M and N are chosen to be 492 and 18, respectively, throughout this analysis.

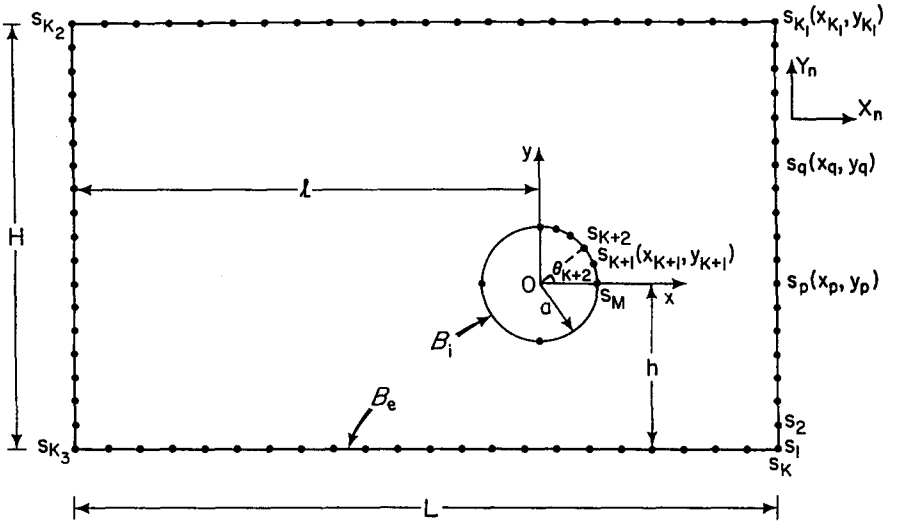

Fig. 3. Collocation points associated with the exterior and interior boundaries of the finite region considered in this study.

$$\left.\begin{aligned} u_r(a, \theta_m) &= -(\delta \cos\theta_m - \lambda) \\ u_\theta(a, \theta_m) &= -\delta \sin\theta_m \end{aligned}\right\} \quad m \in [K+1, K_{\eta_1}] \text{ and } m \in [K_{\psi_1}, M]$$

$$\left.\begin{aligned} u_r(a, \theta_m) &= -(\delta \cos\theta_m - \lambda) \\ |\sigma_{r\theta}(a, \theta_m)| &= f|\sigma_{rr}(a, \theta_m)| \end{aligned}\right\} \quad m \in [K_{\eta_1}+1, K_{\eta_2}] \text{ and } m \in [K_{\psi_2}, K_{\psi_1}-1]$$

$$\sigma_{rr}(a, \theta_m) = 0, \quad \sigma_{r\theta}(a, \theta_m) = 0: \quad m \in [K_{\eta_2}+1, K_{\psi_2}-1] \tag{11}$$

where s_m denotes the location of the collocation point, and the subscript m indicates the index of the collocation points on the exterior and interior boundaries. The indices of the specific collocation points shown in Fig. 3 are chosen as $K_1 = 61$, $K_2 = 123$, $K_3 = 185$, $K = 247$ and $M = 492$. Collocation points defining the slip and no-slip zones are denoted by K_{η_1}, K_{η_2}, K_{ψ_1} and K_{ψ_2}. The coefficient of friction, f, is taken to be 0.2 throughout this study.

The validity of the present analysis is established by comparing the contact stresses determined from this analysis with the experimental measurements reported by Hyer and Liu (1984). In this study, only the results associated with quasi-isotropic $[(0_4^\circ/45_4^\circ/-45_4^\circ/90_4^\circ)_s]$ and unidirectional $[(0_{32}^\circ)]$ laminates with specimen geometry specified as $a = 25.4$ mm, $L = 292$ mm, $H = 203$ mm, $l = 191$ mm, and $h = 101.5$ mm are presented for brevity. In their experimental study, they mentioned a snug fit between the fastener and the hole, i.e. $\lambda = 0$. However, they did not provide the values for pin displacements. Pin displacements corresponding to the applied loads specified in their study were calculated based on the procedure outlined in Appendix B. The comparisons of the contact stresses for these material systems are presented in Figs 4–5. The experimental and analytical predictions correlate extremely well. The experimentally measured and analytically determined contact angles are larger than 180°. This occurs because of the short distance between the pin and the end of the specimen. For specimen configurations with a longer end distance, the contact angle reduces to less than 180°. These stresses are normalized with respect to the bearing stress, σ_B, defined as $\sigma_B = \sigma_0 H/2a$. In order to elucidate the significance of pin displacement, the variation of pin displacement and the corresponding contact area as a function of the applied load are shown in Figs 6 and 7. The non-linear variations shown in these figures belong to the specimen with unidirectional laminates, whose stress distribution around the contact region is depicted in Fig. 5. The material properties for the composite specimens are the same as those specified by Hyer and Liu in their experimental work; the lamina properties are taken to be $E_L = 37.2$ GPa, $E_T = 12.3$ GPa, $G_{LT} = 3.93$ GPa and $\nu_{LT} = 0.3$.

The effect of interaction between the finite boundaries and the off-centered pin-loaded hole on contact stresses and the contact region in anisotropic laminates with lay-up

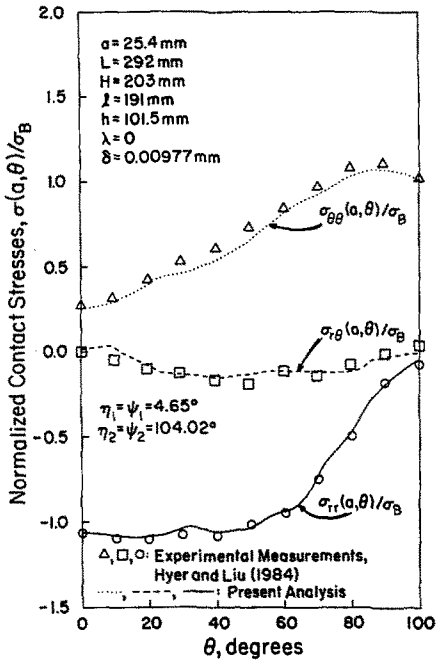

Fig. 4. Stress distribution around the contact region of a pin-loaded hole in a quasi-isotropic laminate.

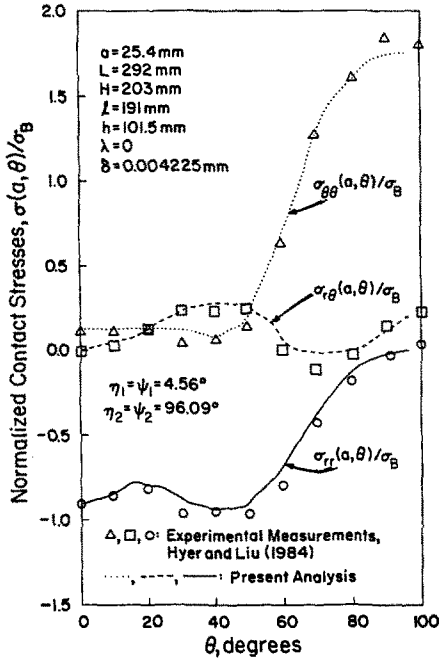

Fig. 5. Stress distribution around the contact region of a pin-loaded hole in a unidirectional laminate.

$(0_5^\circ/\pm 45_2^\circ/90^\circ)_s$ are presented in Figs 8–10.† These figures illustrate the significant increase in stresses when the position of the fastener is close to the edges of the laminate. The rates of increase and their variation shown in Figs 8–10 are specific to the material system considered. Although these results are expected in nature, the individual effects of finite

† The lamina properties of $E_L = 7.8 \times 10^6$ psi, $E_T = 2.6 \times 10^6$ psi, $G_{LT} = 1.3 \times 10^6$ psi and $\nu_{LT} = 0.25$ are used for this and the remaining configurations.

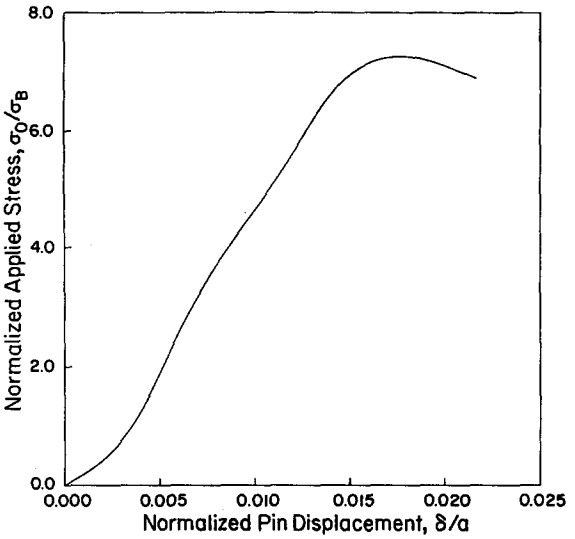

Fig. 6. Variation of pin displacement as a function of applied stress for a pin-loaded hole in a unidirectional laminate.

boundaries and the degree of material anisotropy on the stress distributions are not known *a priori*. The two material systems considered in Figs 4 and 5 illustrate the influence of material anisotropy. The extent of the corresponding no-slip and slip zones of the contact region is also provided in these figures. The asymmetric variation in contact stresses and the increase in contact region become more pronounced when the pin is located near the vertical and horizontal free boundaries. Quantification of the effect of finite geometry on the contact stresses for a specific material system is demonstrated in Figs 8–10. Variation of the contact stresses can be altered by controlling the degree of material anisotropy and pin-hole clearance as a direct consequence of the analysis presented herein.

Orthotropic laminate with two fasteners

The second configuration described in Fig. 1(b) includes two adjacent fasteners located symmetrically and in parallel, but perpendicular to loading, in a finite orthotropic laminate with lay-up $(0°/90°)_s$ so as to account for the effect of finite boundaries, as well as the interaction between the fasteners. Utilizing the symmetry condition with respect to the

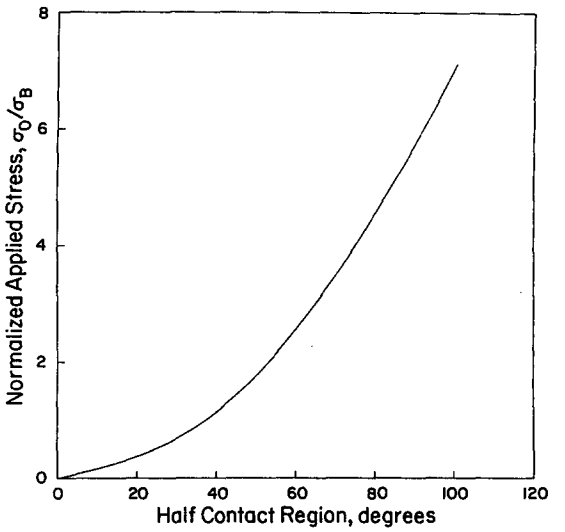

Fig. 7. Variation of contact angle as a function of applied stress for a pin-loaded hole in a unidirectional laminate.

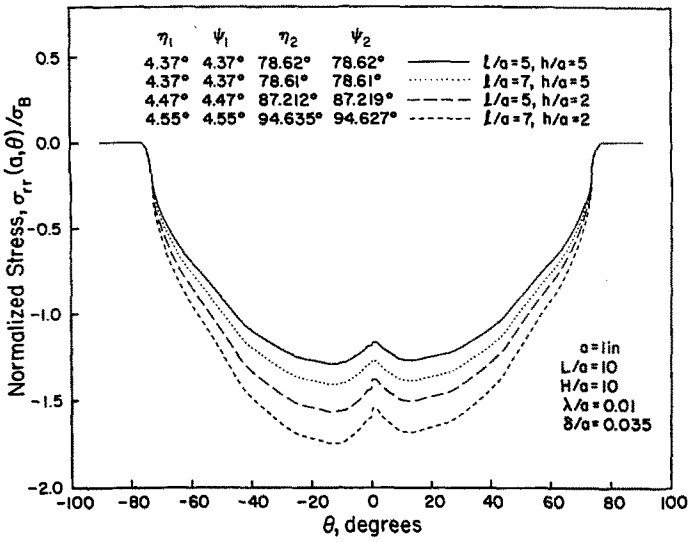

Fig. 8. Radial stresses around the contact region of a pin-loaded hole in a finite anisotropic laminate with a single fastener.

$y = -h$ plane, only one-half of the laminate is considered for the analysis. As shown in Fig. 2, the boundary conditions associated with the collocation points along the exterior boundary, B_e, are specified as:

$$\begin{aligned} &F_x = 0, \quad F_y = 0: && m \in [1, K_1] \\ &F_x = 0, \quad F_y = \sigma_0(H-h): && m \in [K_1+1, K_2] \\ &F_x = \sigma_0(H-h)(s_m+h)/H, \quad F_y = 0: && m \in [K_2+1, K_3] \\ &F_x = 0, \quad u_y = 0: && m \in [K_3+1, K_4]. \end{aligned} \tag{12}$$

The pronounced effects of the interaction between the fasteners on the contact stresses are illustrated in Figs 11–13. These figures also include the stresses for the same size laminate

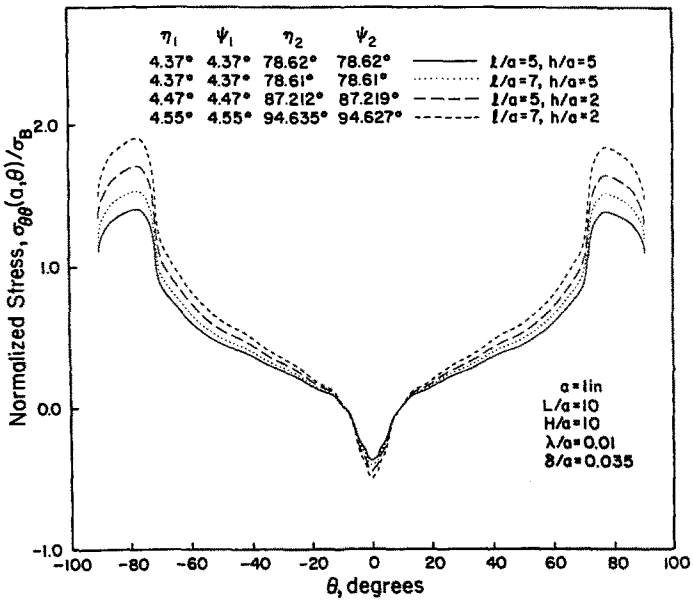

Fig. 9. Tangential stresses around the contact region of a pin-loaded hole in a finite anisotropic laminate with a single fastener.

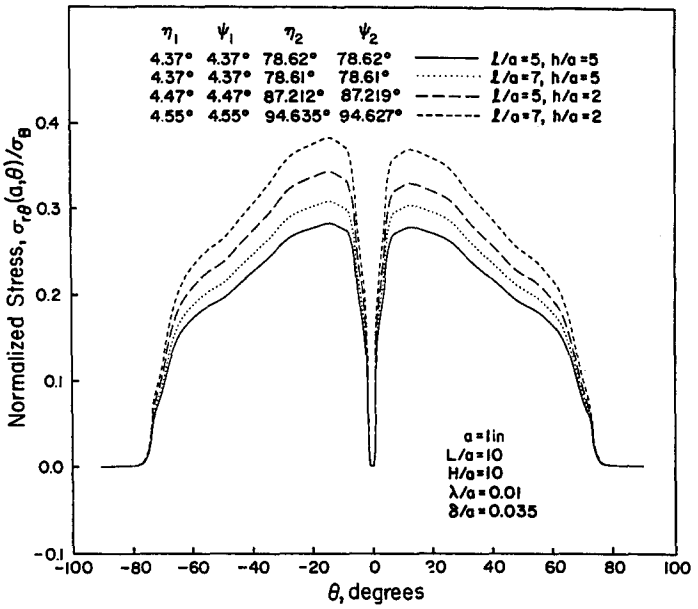

Fig. 10. Shear stresses around the contact region of a pin-loaded hole in a finite anisotropic laminate with a single fastener.

consisting of a single fastener as the base line solution. As expected, the magnitudes of the stresses increase when the distance between the two fasteners decreases. In the case of a commonly accepted design configuration for which $h/a = 3$, the magnitudes of the stresses for two fasteners become considerably higher than those for a single fastener. Again, the extent of the corresponding no-slip and slip zones is given in these figures. Near the ends of the contact region, the radial and shear stresses, although small in magnitude, are not identically zero. Their magnitudes vanish in a continuous manner as the contact region ends.

Orthotropic laminate with a row of fasteners

The third configuration shown in Fig. 1(c) contains a row of fasteners perpendicular to the direction of the applied load. Due to the symmetry conditions along the $y = \pm h$ planes, a finite orthotropic laminate with a single fastener is considered with appropriate

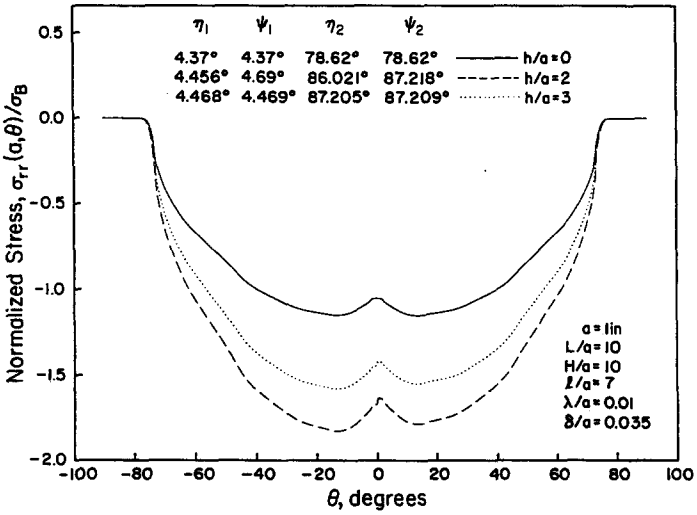

Fig. 11. Radial stresses around the contact region of a pin-loaded hole in a finite orthotropic laminate with two fasteners.

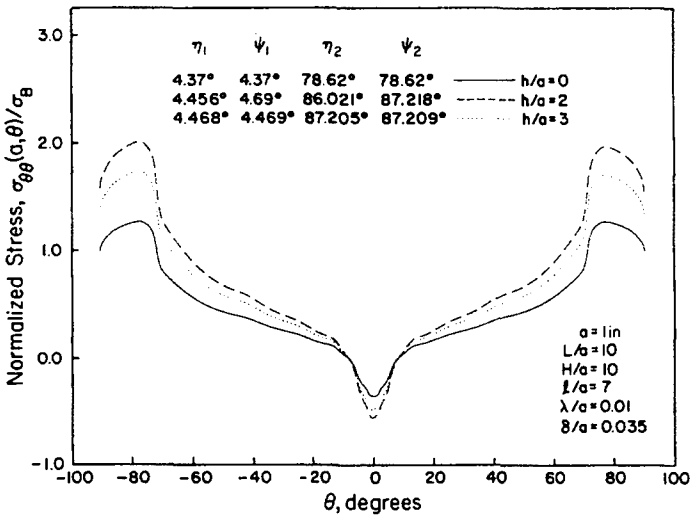

Fig. 12. Tangential stresses around the contact region of a pin-loaded hole in a finite orthotropic laminate with two fasteners.

boundary conditions along these planes. The symmetry conditions require zero shear stresses and the imposition of constant vertical displacements, resulting in zero vertical forces. The appropriate vertical displacements are obtained as part of the analysis by searching for the values that cause the vertical forces to vanish along these planes.

The geometry and loading conditions of this configuration are illustrated in Fig. 1(c). Since $y = \pm h$ are symmetry planes, the boundary conditions imposed on the collocation points along the exterior boundary, B_c, are:

$$\begin{aligned} &F_x = 0, \quad F_y = 0: && m \in [1, K_1] \\ &F_x = 0, \quad v = v^*: && m \in [K_1+1, K_2] \\ &F_x = \sigma_0(H-h)(s_m+h)/H, \quad F_y = 0: && m \in [K_2+1, K_3] \\ &F_x = 0, \quad v = v^*: && m \in [K_3+1, K_4] \end{aligned} \tag{13}$$

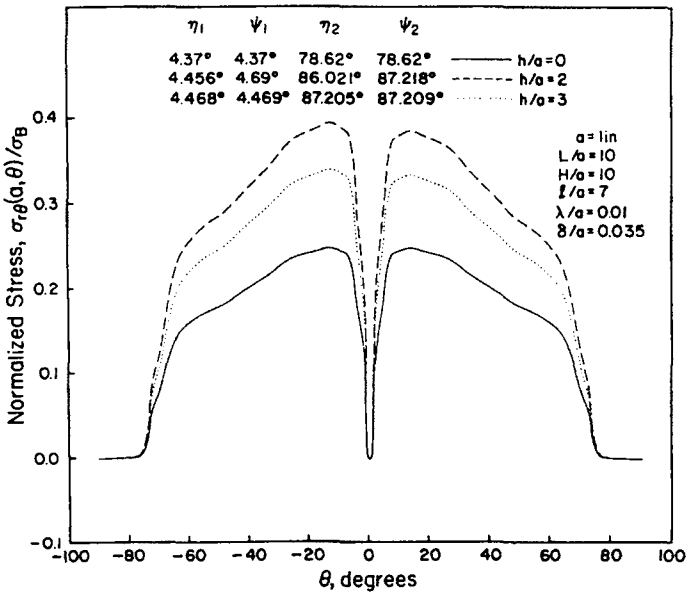

Fig. 13. Shear stresses around the contact region of a pin-loaded hole in a finite orthotropic laminate with two fasteners.

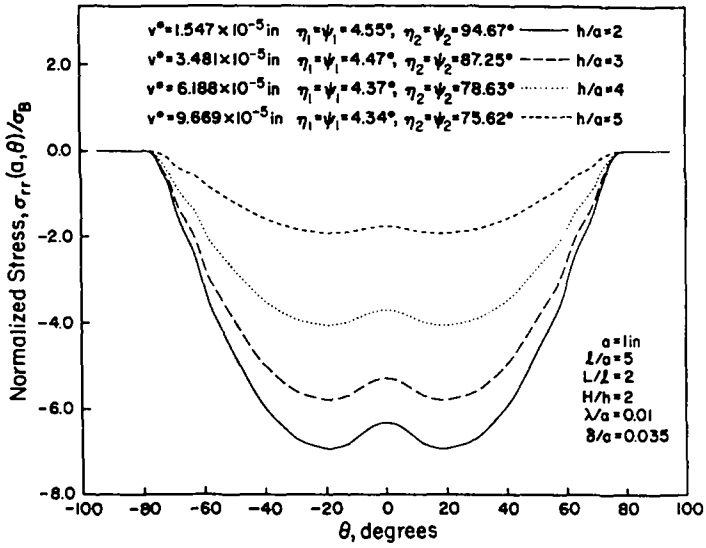

Fig. 14. Radial stresses around the contact region of a pin-loaded hole in an orthotropic laminate with multiple fasteners.

where v^* is calculated as part of the analysis, resulting in zero vertical forces along the symmetry lines. For a specific material system, the effect of spacing between the fasteners on the contact stresses is illustrated in Figs 14–16. As expected, the magnitudes of the stresses become more pronounced as the spacing between the fasteners decreases. However, the amount of increase in these stresses also varies, depending on the material system, pin-hole clearance and friction. The variation of the maximum contact stresses as a function of spacing is presented in Fig. 17. The results shown in these figures are useful in achieving optimum joint configurations based on reduction of the stress concentration.

5. CONCLUSIONS

This study presents an analysis capable of determining the non-linear contact stresses in pin-loaded composite laminates while capturing the effects of finite boundaries, interaction among fasteners, material anisotropy, pin-hole clearance, and friction between the

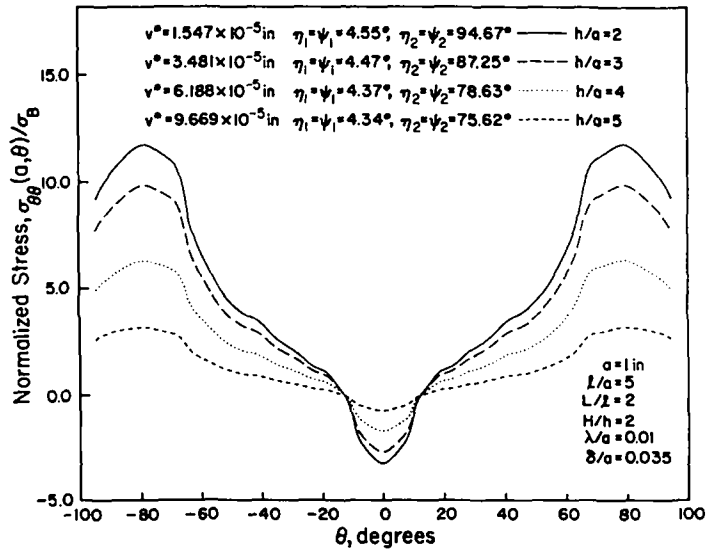

Fig. 15. Tangential stresses around the contact region of a pin-loaded hole in an orthotropic laminate with multiple fasteners.

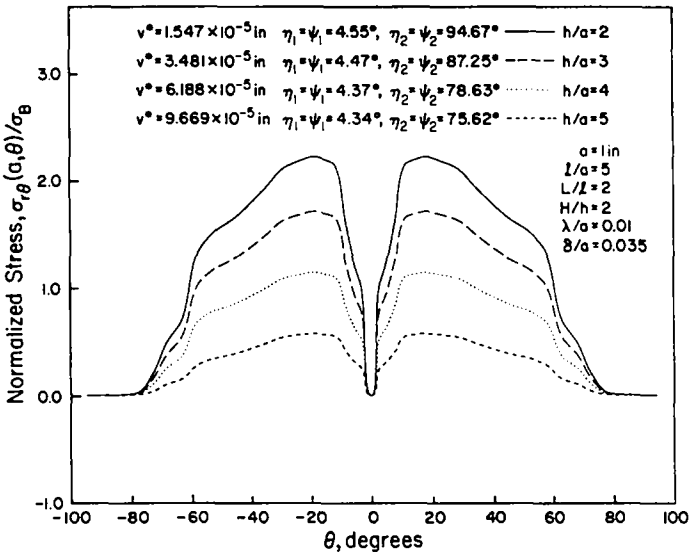

Fig. 16. Shear stresses around the contact region of a pin-loaded hole in an orthotropic laminate with multiple fasteners.

rigid pin and the material. Comparison of the results from this analysis with the experimental photoelastic measurements published by Hyer and Liu (1984) demonstrates the accuracy of the present analysis. Validation of the results involving two or more fasteners was not possible because of the unavailability of experimental measurements in the literature. This is a significant improvement over previous analyses reported in the literature because it provides an accurate basis for selecting material and establishing its stacking sequence without conducting tests, and for evaluating strength prediction models. Furthermore, this analysis can be extended to determine contact stresses in mechanical joints with two or three fasteners in a staggered pattern, including the effect of by-pass loading.

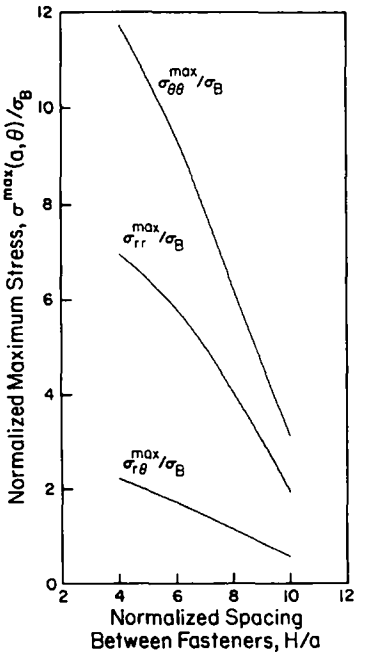

Fig. 17. Effect of spacing between the fasteners on the maximum stresses in the contact region for an orthotropic laminate with a row of fasteners.

REFERENCES

Bowie, O. L. and Neal, D. M. (1970). A modified mapping-collocation technique for accurate calculation of stress intensity factors. *Int. J. Fracture Mech.* **6,** 199–206.

Eriksson, L. I. (1986). Contact stresses in bolted joints of composite laminates. *Composite Struct.* **6,** 57–75.

Eshwar, V. A. (1978). Analysis of clearance fit pin joints. *Int. J. Mech. Sci.* **20,** 477–484.

Horn, R. A. and Johnson, C. R. (1991). *Topics in Matrix Analysis.* Cambridge University Press, Cambridge, U.K.

Hyer, M. W. and Klang, E. C. (1985). Contact stresses in pin-loaded orthotropic plates. *Int. J. Solids Structures* **21,** 957–975.

Hyer, M. W. and Liu, D. (1984). Stresses in pin-loaded plates: photoelastic results. *J. Composite Mater.* **19,** 138–153.

Lekhnitskii, S. G. (1968). *Anisotropic Plates.* Gordon and Breach, New York.

Madenci, E., Ileri, L. and Kudva, J. N. (1993). Analysis of finite composite laminates with holes. *Int. J. Solids Structures* **30,** 825–834.

Mangalgiri, P. D., Dattaguru, B. and Rao, A. K. (1984). Finite element analysis of moving contact in mechanically fastened joints. *J. Nucl. Engng Design* **78,** 303—311.

Marshall, I. H., Arnold, W. S., Wood, J. and Mousley, R. F. (1989). Observations on bolted connections in composite structures. *Composite Struct.* **13,** 133–151.

Murthy, A. V., Dattaguru, B., Narayana, H. V. L. and Rao, A. K. (1990). An improved iterative finite element solution for pin joints. *Computers Struct.* **36,** 1121–1128.

Naik, R. and Crews, J. H., Jr (1986). Stress analysis method for clearance-fit bolt under bearing loads. *AIAA Jl* **24,** 1348–1353.

Naik, R. and Crews, J. H., Jr (1991). Stress analysis method for clearance-fit joints with bearing-bypass loads. *AIAA Jl* **29,** 89–95.

Oplinger, D. W. and Gandhi, K. R. (1974). Stresses in mechanically fastened orthotropic laminates. *Proc. Second Conference on Fibrous Composites in Flight Vehicle Design,* Dayton, Ohio, pp. 813–841.

Rahman, M. V., Rowlands, R. E., Cook, D. E. and Wilkinson, T. L. (1984). Iterative procedure for finite element stress analysis of frictional contact problems. *Computers Struct.* **18,** 947–954.

Ramamurthy, T. S. (1989). New studies on the effect of bearing loads in lugs with clearance fit pins. *Composite Struct.* **11,** 135–150.

Rowlands, R. E., Rahman, T. L., Wilkinson, T. L. and Chang, Y. I. (1982). Single- and multiple-bolted joints in orthotropic materials. *Composites* **13,** 273–279.

Wilkinson, T. L., Rowlands, R. E. and Cook, R. D. (1981). An incremental finite-element determination of stresses around loaded holes in wood plates. *Computers Struct.* **14,** 123–128.

APPENDIX A

The iterative scheme starts with the determination of the η_2 and ψ_2 angles by solving the problem under no-slip conditions, i.e. $\eta_1 = \eta_2$ and $\psi_1 = \psi_2$. Choosing values for η_2 and ψ_2 leads to a solution for the contact stresses in the presence of no friction. If the constraints specified in eqn (2) are not satisfied, the angles defining the no-slip region are adjusted based on the following criteria.

$$\begin{aligned}
&\text{For } R_u > R_L: \eta_2 = \eta_2 - \Delta\eta_2 \quad \text{and} \quad \psi_2 = \psi_2 + \Delta\psi_2,\\
&\text{for } R_u > R_L: \eta_2 = \eta_2 + \Delta\eta_2 \quad \text{and} \quad \psi_2 = \psi_2 - \Delta\psi_2,\\
&\text{for } R_u = R_L \text{ and } R_u + R_L < \sigma_0 H: \eta_2 = \eta_2 + \Delta\eta_2 \quad \text{and} \quad \psi_2 = \psi_2 + \Delta\psi_2,\\
&\text{for } R_u = R_L \text{ and } R_u + R_L > \sigma_0 H: \eta_2 = \eta_2 - \Delta\eta_2 \quad \text{and} \quad \psi_2 = \psi_2 - \Delta\psi_2
\end{aligned} \tag{A.1}$$

where R_u and R_L are the components of the load exerted by the pin on the upper and lower part of the $y = 0$ line, respectively. The incremental angles $\Delta\eta_2$ and $\Delta\psi_2$ are defined by

$$\Delta\eta_2 = \left|\frac{\eta_2^{(i)} - \eta_2^{(i-1)}}{\eta_2^{(i)} + \eta_2^{(i-1)}}\right| \quad \text{and} \quad \Delta\psi_2 = \left|\frac{\psi_2^{(i)} - \psi_2^{(i-1)}}{\psi_2^{(i)} + \psi_2^{(i-1)}}\right| \tag{A.2}$$

where superscript i specifies the sequence of iterations in the solution procedure. With these adjusted values of η_2 and ψ_2, another solution for the contact stresses is obtained and checked against the conditions for convergence given in eqn (2). The angles η_2 and ψ_2 are repeatedly re-adjusted until these conditions are satisfied.

The converged solution obtained for the contact region described only by the no-slip zone provides the first estimate of the angles η_2 and ψ_2, as well as the boundary conditions involving Coulomb friction along the slip zone defined by assumed values for angles η_1 and ψ_1. With these initial values for η_1, η_2, ψ_1, ψ_2, and $\sigma_{rr}(a, \theta)$, the contact stresses are obtained along the no-slip and slip zones. If these contact stresses do not satisfy the conditions for convergence specified by eqn (2). the angles η_2 and ψ_2 are adjusted based on the criteria given by eqn (A.2). The angles defining the slip and no-slip zones are adjusted based on the following criteria.

$$\begin{aligned}
&\text{For } \eta_2^{(i)} > \eta_2^{(i-1)}: \eta_1 = \eta_1 + \Delta\eta_2,\\
&\text{for } \eta_2^{(i)} < \eta_2^{(i-1)}: \eta_1 = \eta_1 - \Delta\eta_2,\\
&\text{for } \psi_2^{(i)} > \psi_2^{(i-1)}: \psi_1 = \psi_1 + \Delta\psi_2,\\
&\text{for } \psi_2^{(i)} < \psi_2^{(i-1)}: \psi_1 = \psi_1 - \Delta\psi_2
\end{aligned} \tag{A.3}$$

in which $\Delta\eta_2$ and $\Delta\psi_2$ are defined by eqn (A.2). With the adjusted values of η_1, η_2, ψ_1 and ψ_2 and the radial

stresses from the previous solution, another solution is obtained for the contact stresses. This process continues until the contact stresses satisfy the condition for convergence.

APPENDIX B

In calculating the pin displacements corresponding to the applied loads used by Hyer and Liu (1984) in their experimental work, the following procedure is adopted.

(1) Determine the first estimate of the contact region (P and S) corresponding to the specified load by assuming a value for the pin displacement, δ.
(2) Compute the displacement component, $u_x(x = -a, y = 0)$ corresponding to the specified load by imposing zero displacement conditions along the first estimate of the contact region.
(3) By setting $\delta = u_x(x = -a, y = 0)$, calculate another estimate of the contact region as in Step 1 and compute the displacement component, $u_x(x = -a, y = 0)$ corresponding to this contact region as in Step 2. Repeat this process until the difference between the consecutive pin displacements is less than or equal to 10^{-5}.